JOURNAL OF BIOMEDICAL OPTICS 1(1), 98–109 (JANUARY 1996)

PHOTOPHYSICAL PROPERTIES OF FLUORESCENCE PROBES I: DIALKYLAMINO STILBAZOLIUM DYES

Bernd Strehmel and Wolfgang Rettig
Humboldt-Universität zu Berlin, Institut für Physikalische und Theoretische Chemie, Bunsenstr. 1, D-10117 Berlin, Germany

(Paper JBO-023 received July 24, 1995; revised manuscript received Nov. 13, 1995; accepted for publication Nov. 16, 1995)

ABSTRACT

The photophysical and photochemical behavior of different isomers of dimethylamino-stilbazolium dyes was investigated in *n*-alcohols at different temperatures by stationary and time-resolved fluorescence measurements. At room temperature, an efficient nonradiative deactivation k_{nr} was observed, which increases in high-polarity and low-viscosity solvents. For viscosities $\leqslant$ 10 cP, k_{nr} possesses a linear viscosity dependence. At low temperatures, the fluorescence spectra show considerable blue shifts, which are absent in solvent polarity changes relative to room temperature, and a spectral narrowing. From the combined quantum yield and lifetime measurements, k_{nr} is shown to decrease strongly with decreasing temperature, by more than two orders of magnitude, and k_f is shown to increase. These facts and the observation of an initial lifetime lengthening by increasing the temperature from 77 K indicate several simultaneously emitting states with a temperature-dependent population efficiency. These states were tentatively assigned to several possible single-bond twisted excited conformers. This assignment is supported by the near absence of isomerization.

Key Words fluorescence probe, styryl compound, adiabatic photoreaction, multiple fluorescence, free volume.

1 INTRODUCTION

Substituted stilbazolium salts exhibit a very strong temperature-dependent fluorescence quantum yield above the glass transition temperature of polymers and ordinary solvents.[1–5] This phenomenon of a medium dependent fluorescence was observed for these compounds[4–6] and investigated for other fluorescing species such as triphenylmethane dyes.[7,8] In general, it offers many applications in different fields of science.[1,2]

Some of these applications exist in medicine where these and related dyes are used as fluorescence indicators in neurons[9] because they exhibit a strong charge shift[10] upon light excitation. Moreover, this property can also be used to detect differences in membrane potentials[10,11] of biological materials. Some of the results reported in these works[10,11] were obtained in membranes and lipid bilayers, and they were compared with data measured in common isotropic solvents. The authors[10] discuss their results on the basis of a differential solvation model, which can yield increased importance in organized systems. It was also reported that the solvent-dependent change of the spectra[11] was applied as a fit parameter in studies of the voltage sensitivity of several hemicyanine dyes in membranes.

In general, viscosity-dependent fluorescence can be used to construct fluorescence probes usable during the control of the synthesis of polymer composites[3,8] or to get information about the microscopic properties of the molecular surrounding.[3,6–11] For a deeper understanding, the photochemistry of the probe molecule should be well understood. Then, it is possible to correlate quantitative fluorescence measurements on the probe molecule with specific material properties of the medium.

Triphenylmethane dyes were successfully used for such investigations.[7] However, these dyes present disadvantages in some practical applications because of their chemical reactivity with bases or nucleophiles that are part of a given matrix. The stilbazolium dyes investigated in this work are chemically much less reactive because the pyridinium group in the acceptor part of the styryl dye possesses lower electrophilic properties than charged triphenylmethane dyes. On the other hand, the fluorescence probe properties of these compounds are more complex because both fluorescence maximum and quantum yield change with increasing viscosity of the surrounding matrix.[5]

Address all correspondence to Bernd Strehmel. E-mail: bernds@asterix.chemie.hu-berlin.de

The goal of this work is a better understanding of the photophysical properties of the stilbazolium dyes, especially in relation to their usefulness in describing viscosity or temperature-dependent effects in different materials. The photophysics of 4-dialkylamino-4′-azastilbenes was investigated earlier with stationary fluorescence measurements, isomerization experiments and pulse radiolysis.[5] An important property, the simultaneous dependence of photophysics on solvent viscosity and polarity, was found for stilbazolium and related pyridinium dyes by Fromherz and co-workers.[4,12,13] These authors discuss the results by invoking single-bond twisting in the excited state toward a "twisted intramolecular charge transfer" (TICT) state[14–16] as the main cause for these dependencies and also for the very short fluorescence lifetimes in dilute solutions at room temperature. Incidentally, the short fluorescence lifetime in low-viscosity solvents is an important factor in the use of these compounds as mode locking dyes.[17]

In view of the results of the model compound studies on donor-acceptor stilbenes,[18–21] which reveal fluorescence from twisted species, we asked whether such behavior could also be observed for the stilbazolium dyes, under low-temperature conditions. As these dyes possess several flexible single bonds, several TICT products can in principle be expected and should be accessible from the initially reached first excited singlet state.[4] This is demonstrated here by the observation of an anomalous temperature dependence of the fluorescence lifetimes. This effect, a lifetime maximum in the region of the glass transition temperature T_g of the solvent,[22] was also observed for nonionic donor-acceptor stilbenes.[18] Multiple fluorescence is furthermore supported by the strong temperature dependence of the fluorescence halfwidths.

The paper is organized in the following way: The three positional isomers of dimethylaminostyrylpyridinium salt are described and compared with respect to their photophysical properties at room temperature. The next section compares the low-temperature fluorescence spectra, quantum yields and lifetimes, and demonstrates the temperature dependence of nonradiative as well as radiative decay processes. The latter can only be understood within a model of several emitting states. As new evidence for multiple emissions, we demonstrate that the formal radiative rate $\Phi_f/\tau_f = k_f$ is temperature dependent, it increases with decreasing temperature in the low-temperature region. The strongly temperature- and viscosity dependent nonradiative channel k_{nr} is therefore also linked to several emissive states.

In a subsequent paper,[23] the theoretical model of TICT states is used in conjunction with theoretical calculations to find out which flexible bonds are most probably involved in the product formation. This model is then applied in a global analysis of the flourescence decays dependent on emission wavelength, and the emission spectra of three species are extracted by this technique.

2 EXPERIMENTAL

2.1 COMPOUNDS

The dyes *trans*-4-(4-dimethylaminostyryl)-1 methylpyridiniumiodide (*p*-DASPMI) and *trans*-2-(4-dimethylaminostytyl)-1-methyl-pyridiniuiodide (*o*-DASPMI) and all solvents (methanol, ethanol, *n*-propanol, *n*-butanol, *n*-hexanol, *n*-octanol, and *n*-decanol) used for the measurements were purchased from Aldrich. The laser dye rhodamine 101 was obtained from Lambda Physik (Göttingen).

The meta derivative *trans*-3-(4-dimethylaminostyryl)-1-methylpyridiniumiodide (*m*-DASPMI) was synthesized by reaction of β-picoliniummethyliodide (obtained by alkylation of β-picoline with methyliodide) and *p*-dimethylaminobenzaldehyde. A total of 4.5 g (0.03 mole) *p*-dimethylaminobenzaldehyde, 9.2 g (0.039 mole) β-picoliniummethyliodide and 3 ml dried piperidine in 90 ml ethanol (abs.) were stirred at 90 °C for 64 h. The red solution obtained was evaporated in vacuum at about 20 mbar and 50 °C until a red solid residue was obtained. The product mixture was cooled down to 5 °C. The solid mass obtained was collected on a Büchner funnel. Nonreacted aldehyde was removed by extraction with bisulfite solution. The raw product was dried in vacuum and purified by recrystallization from water [elementary analysis: C (%)=52.58 (52.47), H (%)=4.97 (5.23), N (%)=7.23 (7.65), yield: 30%].

2.2 MEASUREMENTS

Absorption spectra were measured with a M40 spectrometer (Carl Zeiss Jena AG) and a UV-210 A from Shimadzu. Fluorescence spectra were recorded with a Perkin-Elmer 650-60 fluorimeter. All emission spectra were measured with a spectral bandwidth of 5 nm. The spectra were measured using 1-cm quartz cuvettes, and the emission was detected in perpendicular geometry. Temperature-dependent measurements were carried out with equipment described earlier.[24] The relative accuracy of the temperature was better than 0.5 K. Fluorescence quantum yields were measured relative to rhodamine 101 in ethanol (Φ_f=1.0).[25] All spectra were corrected by using the correction procedure described earlier.[26]

2.2.1 Fluorescence Lifetime Measurements

Two kinds of pulsed light sources were used to determine the fluorescence lifetimes τ_f.

a. Mode-locked Ar-ion laser

The experimental setup was described in detail earlier.[27] A mode-locked argon ion laser (Carl Zeiss Jena AG) was used to produce light pulses with a

lifetime of about 80 ps and a repetition frequency of 125.1 MHz at the excitation wavelength of 476 nm. The detection system consisted of a standard single-photon counting setup.[28] The apparatus response function (300 ps FWHM with an 18 ELU-FM photomultiplier) was determined with pinacyanol in ethanol. More details about electronic and optical components were described in a previous work.[29] The achievable time resolution was 50 ps[29] (with iterative reconvolution). λ/4 plates from LOT (Darmstadt) were used to eliminate polarization effects. Temperature control was achieved with a cryostat TSK 200 from the former East German Academy of Sciences (relative accuracy of temperature better than 1 K).

b. Synchrotron radiation

Fluorescence lifetime measurements were performed at the Berlin storage ring for synchrotron radiation (BESSY) in the single bunch mode (4.8 MHz repetition rate)[24,30] using single-photon counting detection.[28] By means of an excitation monochromator (20-cm focal length, Jobin Yvon) the excitation wavelength was selected from the spectral continuum of the synchrotron radiation. The pulses had a halfwidth of 500 ps. Standard electronics from ORTEC was used for the time-correlated single-photon counting technique and the emission wavelength was selected using a similar monochromator (bandwidth 20 nm). A microchannel plate photomultiplier (Hamamatsu R1564-U-01) cooled to −25 °C was taken for the detection. The achievable time resolution was about 0.1 ns. Further details were described in previous publications.[7,24,30]

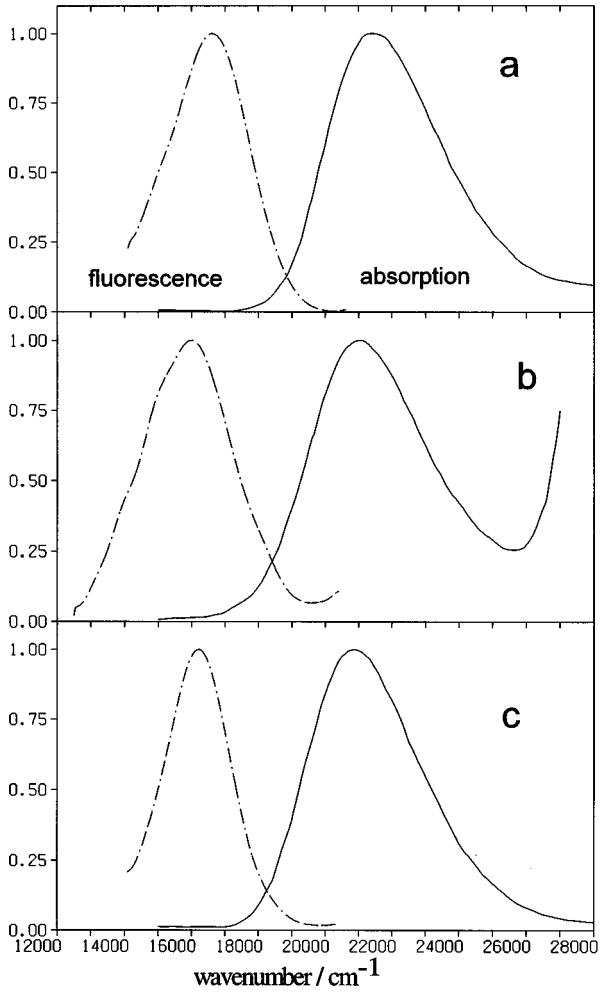

Fig. 1 Normalized absorption and fluorescence spectra for the three DASPMI isomers in ethanol at room temperature, a, *o*-DASPMI; b, *m*-DASPMI; c, *p*-DASPMI.

2.2.2 Quantum Chemical Calculations

Energy gaps between ground and excited states have been calculated by the complete neglect of differential overlap (CNDO/S) method of Del Bene and Jaffé[31,32] using the QCPE program #333 with the original parameters, but modified to cope with larger molecules and to calculate excited-state dipole moments and charge distributions. Standard geometries were used[33,34] (bond lengths R(C—C) =1.40 Å, R(C—H) 1.083 Å, angles 120 degrees) except for the ethylenic bond [R(C═C)=1.33 Å] and the adjacent single bonds [R(C—C)=1.45 Å], angle 128 degrees. The DASPMI isomers were generated from the stilbene skeleton[34] by replacing hydrogen with the different substituents: dimethylamino [$R(C_{ar}—N)$=1.37 Å, $R(N—CH_3)$=1.46 Å], angles 120 degrees with tetrahedral CH_3 groups [R(C—H) =1.083 Å]. For the hetero ring in the DASPMI derivatives, the same regular hexagon was used, with the exocyclic methyl group at R(C—C)=1.46 Å. The planar geometry assumed all dihedral angles as zero (double bond twist angle φ and the twist angles of phenyl and dimethylamino).

3 RESULTS AND DISCUSSION

3.1 ROOM TEMPERATURE RESULTS

The absorption and fluorescence spectra of *o*-, *m*- and *p*-DASPMI are plotted in Fig. 1. The corresponding chemical structures are shown in Scheme 1. With respect to the absorption, a strongly red-shifted fluorescence was measured for all three isomers: Stokes shifts of 4955 cm^{-1} for ortho, 5083 cm^{-1} for meta, and 4606 cm^{-1} for the para compound in ethanol. Such values are unusually large relative to comparable ionic dyes like rhodamine, triphenylmethane and cyanine compounds, which possess values at around 1000 cm^{-1} and lower.[35] Moreover, rhodamines and cyanines possess bands with halfwidths around 700 to 800 cm^{-1} [35] whereas the DASPMI isomers display bandwidths between 2200 and 3200 cm^{-1}. The large Stokes shifts and halfwidths for the DASPMI derivatives are readily understandable (Table 1) within a model involving

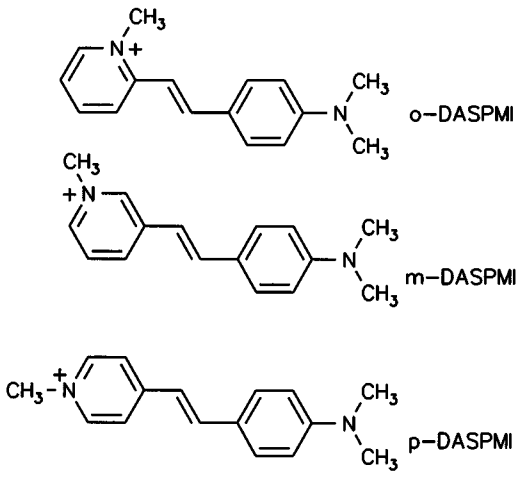

Scheme 1. Structural formulas of the DASPMI isomers.

adiabatic photochemical reactions and multiple fluorescence.

The experimental values of the absorption spectra are compared in Table 1 with those calculated by the CNDO/S method for the planar conformation and a fairly good agreement is found. Noteworthy is the case of *m*-DASPMI where the calculations are in line with the reduced molar extinction coefficient measured. This "meta-effect" is similarly found in neutral dyes such as dimethylaminonitrostilbenes.[21]

The rate constant for the natural fluorescence k_{fn} was calculated from the absorption spectra according to Eq. (1):[36]

$$k_{fn} = 4.32 \cdot 10^{-9} \cdot \epsilon_{max} \cdot \nu_{max}^2 \cdot \Delta\nu_{1/2}\,, \qquad (1)$$

where ν_{max} = absorption maximum, ϵ_{max} = maximum of the molar absorption coefficient, and $\Delta\nu_{1/2}$=halfwidth of the absorption band.

It can be seen that the data calculated with Eq. (1) possess the lowest value for the meta compound, due to the lowered molar absorption coefficient of this isomer. The data thus obtained were compared with the experimental k_f values determined from fluorescence quantum yields and lifetimes [Eq. (2)]:

$$k_f = \frac{\phi_f}{\tau_f}. \qquad (2)$$

The results obtained are summarized in Table 1. The values obtained are not exactly identical but both columns of k_f and k_{fn} show the same tendency: the values for the meta compound are lower than for the ortho as well as the para isomer.

Interestingly, the *m*-DASPMI derivative possesses the fastest nonradiative deactivation rate and the lowest fluorescence quantum yield. This is similar to the corresponding *m*-nitrostilbene derivative[21] and may be related to two causes: (1) a reduced k_f value for the meta compared with the ortho and para compounds, as indicated by the results in Table 1, and (2) an especially reduced energy gap between S_1 and S_0 for the double-bond twisted species P* in the case of the meta compound (see also the theoretical results contained in a subsequent paper[23]).

The results in Table 1 indicate very low fluorescence quantum yields Φ_f and fluorescence lifetimes τ_f at room temperature, due to nonradiative deactivation k_{nr} , which can be due either to the twisting of the double bond,[18] or to triplet formation. k_{nr} can be quantified by Eq. (3). This treatment is a simplification that assumes monoexponential decays or average lifetimes, and it is applicable only for highly efficient nonradiative processes.

$$k_{nr} = \frac{(1-\Phi_f)}{\tau_f}. \qquad (3)$$

For a better understanding of the photophysical details, the fluorescence behavior of *o*-DASPMI was investigated more closely in homologous *n*-alcohols at room temperature. The results are collected in Table 2 together with the viscosities η and dielectric constants ϵ of the solvents.

The absorption maximum varies only slightly with a change of solvent properties. The shift of the

Table 1 Calculated and experimental absorption data and measured fluorescence data of the DASPMI isomers in ethanol at 298 K.

	ν_{max}^{abs}	ν_{max}^{abs}	ν_{max}^{flu}	$\log\epsilon_{max}$	$\log\epsilon_{max}$	Φ_f	τ_f [b]	k_{nr}	k_{fn}	k_f [b]
Compound	cm^{-1} calc[a]	cm^{-1} exp	cm^{-1}	exp	calc[a]		ns	$10^8\ s^{-1}$	$10^8\ s^{-1}$ calc	$10^8\ s^{-1}$ exp
o-DASPMI	23288	21505	16550	4.56	4.51	0.008	0.034	29.1	2.42	2.35
m-DASPMI	21266	21053	15970	3.88	4.05	0.001	<0.020	49.9	0.48	>0.50
p-DASPMI	23602	20876	16270	4.51	4.63	0.008	0.051	19.4	1.74	1.57

[a] Calculated using CNDO/S-CI for planar geometry.

[b] Experimental error ±50% because of the limited time resolution of the time-correlated single-photon counting equipment.

Table 2 Photophysical and spectral data for o-DASPMI determined in different *n*-alcohols at room temperature (298 K).

		η^a			τ_f	k_{nr}	ν_{abs}^{max}	ν_{flu}^{max}
Solvent	Abbreviation	mPa s^{-1}	ϵ^a	Φ_f	ns	10^9 s^{-1}	cm^{-1}	cm^{-1}
methanol	MeOH	0.057	32.7	0.006			21645	16339
ethanol	EtOH	1.678	24.5	0.008	0.034	29.1	21598	16611
n-propanol	PrOH	1.947	20.3	0.017	0.116	8.50	21321	16778
n-butanol	BuOH	2.607	17.5	0.026	0.160	6.10	21231	16807
n-hexanol	HeOH	4.592	13.3	0.047	0.380	2.50	21413	16835
n-octanol	OcOH	7.215	9.8	0.080	0.450	2.00	21413	17123
n-decanol	DeOH	11.800	8.1	0.098	0.620	1.67	21512	16977

[a] Solvent data were taken from Ref. 4.

fluorescence maximum is slightly more dependent on the alcohols used but the overall changes in the Stokes shift $\Delta|\nu_A-\nu_F|$ (from methanol to decanol) remain below 1000 cm^{-1}. A similar solvent dependence on alcohols was also described on previous studies.[4,5]

The influence of the alcohol chain length is, however, strong on both fluorescence quantum yield and lifetime, which change by a factor of more than 10. This is due to the nonradiative decay rate k_{nr}. The solvent influence on the radiative properties of *o*-DASPMI was studied by estimating the fluorescence rate constant k_f. This value can be determined by plotting Φ_f versus τ_f according to Eq. (4) (see Fig. 2);

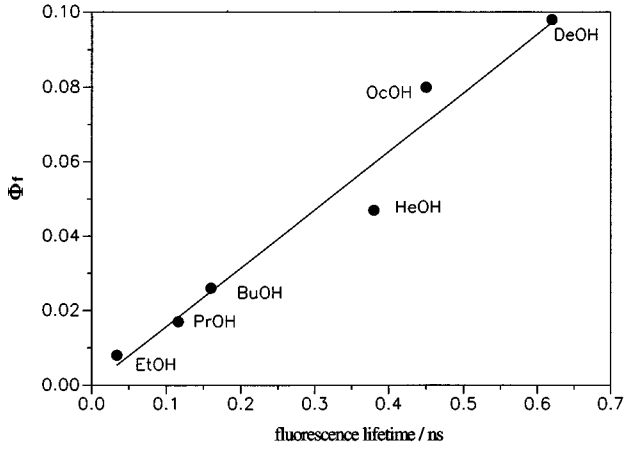

Fig. 2 Dependence of the fluorescence quantum yield on the fluorescence lifetime [according to Eq. (4)] for *o*-DASPMI in different aliphatic alcohols at room temperature (r=0.971; error: 12%).

$$\Phi_f=\frac{k_f}{k_f+k'_{nr}+k_{rot}(T,\eta)}=k_f\cdot\tau_f, \tag{4}$$

where k'_{nr} = viscosity-independent, nonradiative rate constant and k_{rot} = a viscosity-dependent, nonradiative rate constant.

From the slope of the straight line, the fluorescence rate constant k_f was obtained as $1.6\cdot10^8$ s^{-1}. This value is in good agreement with results published by Ephardt and Fromherz[4] for a related para-substituted styryl compound. In addition, the observed linear relationship indicates that k_f does not change significantly at room temperature in different alcohols.

The strongly viscosity-dependent nonradiative rate constant k_{nr} (Table 2; k_{nr} is an overall constant that contains both viscosity/temperature-dependent k_{rot} and temperature-independent k'_{nr} processes) indicates that the viscosity-independent part of k_{nr} is negligible, and we may put $k_{nr}(\eta,T)=k_{rot}(\eta,T)$. The rate constant k_{rot} corresponds to the strong viscosity-dependent intramolecular rotational motion around flexible bonds. This behavior of the probe molecule leads to nonemissive funnels in the excited state. Furthermore, Eq. (5) has been often used to describe the quantitative dependence of k_{nr} on the macroscopic viscosity η, and it is a reasonable basis for explaining intramolecular quenching processes in probe molecules by the medium.

$$k_{nr}=C\,\eta^{-\gamma}. \tag{5}$$

The exponent γ describes the dependence of the nonradiative rate constant k_{nr} on the macroscopic solvent viscosity.[3,7,27] A γ value of 1 indicates that the relaxation behavior of the dye is inversely proportional to the macroscopic viscous flow of the sol-

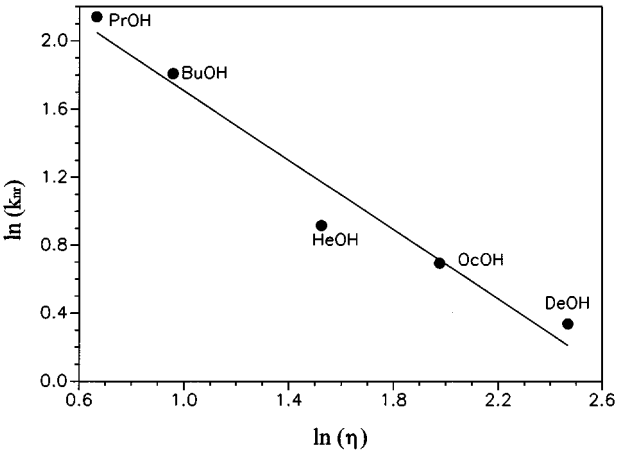

Fig. 3 Dependence of the rate constant k_{nr} on the macroscopic viscosity η [logarithmic plot in accordance with Eq. (5); k_{nr} was evaluated from photophysical data] for *o*-DASPMI in different aliphatic alcohols at room temperature (r=0.963; error: 15%).

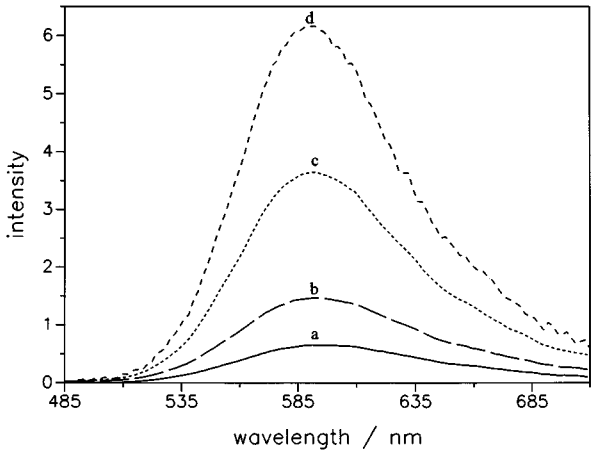

Fig. 4 Fluorescence spectra for *o*-DASPMI at different temperatures in ethanol. a, 298 K; b, 273 K; c, 243 K; d, 228 K. Whereas the fluorescence intensity changes drastically, the maximum remains approximately constant.

vent molecules. On the other hand, γ values smaller than 1 indicate the presence of microviscosity effects.[3,7,27] In Fig. 3 the logarithmic values of k_{nr} are plotted versus the logarithm of η to determine the γ value according to Eq. (5). A relatively good straight line was obtained with a slope around −1. This result, γ=1, indicates that for the dyes investigated, microviscosity effects are not important at room temperature.

The k_{nr} values are rather close to the rate constants for the solvent longitudinal dielectric relaxation k_{dl}[37] (ethanol: $k_{dl}=33\cdot10^9$ s^{-1}, $k_{nr}=29\cdot10^9$s^{-1}; *n*-propanol: $k_{dl}=12\cdot10^9$ s^{-1}, $k_{nr}=9\cdot10^9$ s^{-1}; *n*-butanol: $k_{dl}=8\cdot10^9$ s^{-1}, $k_{nr}=6\cdot10^9$ s^{-1}). This result may indicate that solvation kinetics around an intramolecular charge transfer state is an important factor, too. These dyes can therefore be used as probes for changes in both viscous and dielectric relaxation properties, for different applications in medicine,[9] biology,[10,11,38] nonlinear optics[39] and polymer chemistry.[3,40,41]

3.2 LOW-TEMPERATURE SPECTROSCOPY

Fluorescence lifetime and quantum yield measurements carried out in various solvents or polymer matrices using the DASPMI isomers at different temperatures provide a useful approach to obtaining specific material properties such as microviscosity, mobility, and the free volume.[3,7,8,27] However, the photochemical and photophysical processes of the probe need to be known in detail for a quantitative interpretation of the fluorescence experiments. Therefore, we studied the fluorescence behavior of the DASPMI isomers at different temperatures in ethanol to obtain quantitative information on the changes of the fluorescence rate constant k_f and the efficiency of the nonradiative processes. A possible temperature dependence of k_f can give information on the nature of emissive state(s).

The results obtained by stationary fluorescence measurements are shown in Figs. 4 and 5 for the ortho isomer investigated. In the temperature region from 298 to 108 K, an increase of the fluorescence intensity (Φ_f) was found with decreasing temperature or increasing viscosity in ethanol. This effect can be caused by a reduction of k_{rot} in Eq. (4) due to increased solvent viscosity. As a result, the fluorescence quantum yield changes strongly, but the maximum does not vary with increasing viscosity in the temperature region from 298 to 228 K (viscosity range from 1 to 10 cP). With a further increase of solvent viscosity, especially at temperatures around the glass transition temperature

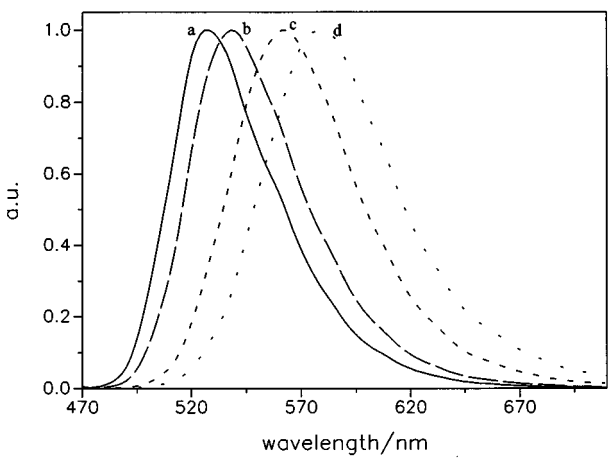

Fig. 5 Normalized fluorescence spectra of *o*-DASPMI measured at different temperatures in ethanol. a, 108 K; b, 123 K; c, 143 K; d, 163 K.

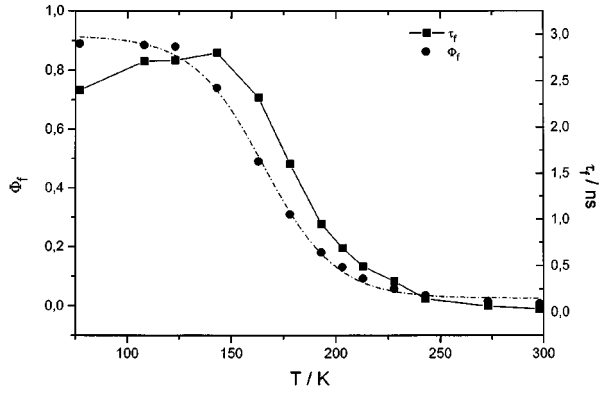

Fig. 6 Dependence of fluorescence quantum yields and fluorescence lifetimes for *o*-DASPMI at different temperatures in ethanol (measured at the fluorescence maximum; for exact data for maxima, see Table 3).

T_g (≈150 K) and below, the maximum of the spectra starts to shift into the blue region (Fig. 5).

The absence of a temperature-induced shift above 200 K and the strong blue shift below 160 K are an indication for the existence of more than one emitting species with somewhat different emission maxima. Furthermore, we have not found any indications in the excitation spectra for the existence of more emitting ground-state conformers. Therefore, we can conclude that the changing fluorescence measured is caused by different conformers in the excited state, which are formed during an adiabatic photoreaction. The variation of the viscosity in the low-temperature region changes the proportion of these states because the population depends differently on temperature/viscosity. On the other hand, in the lower viscosity region (temperature range from 298 to 228 K), the composition of the species has reached an equilibrium, and the nonradiative deactivation of the ensemble of species dominates.

The fluorescence quantum yields and average lifetimes are plotted as a function of temperature in Fig. 6 for *o*-DASPMI. Φ_f increases with decreasing temperature and reaches a plateau in the glassy state. In the frozen solvent ($T<150$ K), where intramolecular rotation does not dominate, a Φ_f of about 0.9 was determined for *o*-DASPMI.

The corresponding plot of the τ_f values versus temperature shows an anomalous lifetime maximum at around 150 K, i.e. in the temperature region where the strong blue shift starts (see Fig. 5).

The definition of the fluorescence lifetime [Eq. (6)] is used for further discussions:

$$\tau_f = \frac{1}{k_f + k'_{nr} + k_{rot}(T,\eta)} . \qquad (6)$$

At low viscosities, $k_{rot}(T,\eta)$ is large compared with k_f and k'_{nr} and very low Φ_f and τ_f values result (compare the discussion about fluorescence behavior at room temperature above). With increasing viscosity, $k_{rot}(T,\eta)$ decreases, and in the same way τ_f increases to 150 K. However, the decrease of the fluorescence lifetime below 150 K can only be explained on the basis of Eq. (6) if k_f also depends on temperature.

As k_f is an effective value, i. e. the weighted sum of all radiative processes, the anomalous temperature behavior of τ_f can be understood by assuming several emitting species the proportion of which changes such that k_f increases with decreasing temperature. The experimentally obtained k_f values as calculated from the measured Φ_f and τ_f values according to Eq. (2) indeed show such a temperature dependence. For *o*-DASPMI, the change of k_f amounts to a factor of about 2 (Fig. 7).

The dependence of k_f on temperature can be explained with the change of the major component of the emission from a more allowed state ($k_f = 3.7 \cdot 10^8$ s^{-1} at 77 K) to an equilibrium of less allowed ones (k_f ca. $1.7 \cdot 10^8$ s^{-1}) at room temperature. The meta and para isomers of DASPMI exhibit a similar temperature dependence. The results are summarized in Tables 3 to 5.

In some cases, the blue shift of the fluorescence maxima with decreasing temperature has been interpreted with a model based on the relaxation of solvent dipoles.[6,42,43] For strongly dipolar species, e.g. the TICT state of dimethylaminobenzonitrile,[44,45] or in donor-acceptor biphenyls,[46] the emission usually shifts to the red in aprotic po-

Table 3 Photophysical and spectroscopic data for *o*-DASPMI in ethanol at different temperatures.

T		τ_f	k_f	k_{nr}	ν_{max}^{flu}	$\nu_{1/2}^{flu}$
K	Φ_f	ns	10^8 s^{-1}	10^6 s^{-1}	cm^{-1}	cm^{-1}
298	0.008	0.034	2.35	29100	16550	2850
273	0.016	0.064	2.5	15300	16720	2675
243	0.035	0.142	2.465	6770	16810	2501
228	0.057	0.33	1.727	2840	16810	2369
213	0.092	0.49	1.878	1830	16870	2268
203	0.13	0.69	1.884	1240	16950	2268
193	0.18	0.95	1.895	840	16950	2210
178	0.31	1.6	1.938	407	17070	2152
163	0.49	2.32	2.112	194	17190	2036
143	0.74	2.8	2.643	60	17710	2094
123	0.88	2.72	3.235	4.1	18540	1995
108	0.88	2.71	3.372	4.3	18880	1978
77	0.88	2.4	3.708		19230[a]	

[a] Value was estimated from literature data (Ref. 5).

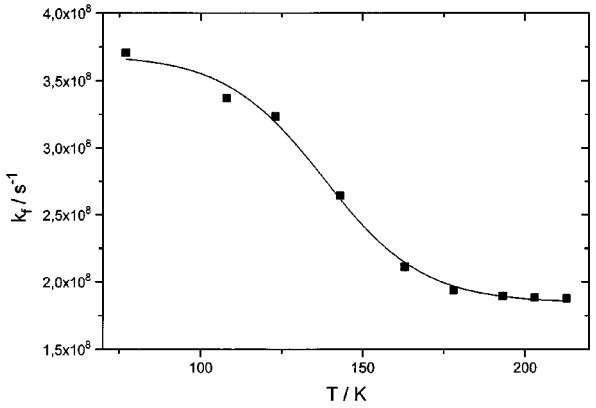

Fig. 7 Dependence of the radiative rate constant k_f for *o*-DASPMI in ethanol at different temperatures.

lar solvents upon lowering the temperature because the effective polarity increases. If, however, solvent relaxation is incomplete within the excited-state lifetime, the spectra shift to the blue. This is the case in alcoholic solvents below room temperature[46] due to their comparatively slow dielectric relaxation times.

The following effects reported here disagree with the solvent relaxation model:

1. The DASPMI compounds show very little blue shift in the temperature region 298 to 190 K, where dipolar dyes show a distinct blue shift. This is consistent with a minor contribution of dipolar relaxation in the case of the DASPMI derivatives and in line with the small solvatochromic shifts observed in the room temperature experiments. The strong blue shift observed at 160 K and below is therefore due to a different origin.
2. The decrease of the halfwidths $\Delta\nu_{1/2}$ of the fluorescence spectra at low temperatures, as plotted in Fig. 8 for *o*-DASPMI, indicates that the spectra narrow considerably at low temperatures. This result is consistent with data for other molecules[46] where the changes in spectral shape were discussed within a model

Table 4 Photophysical and spectroscopic data for *m*-DASPMI in ethanol at different temperatures.

T		τ_f	k_f	k_{nr}	ν_{max}^{flu}	$\nu_{1/2}^{flu}$
K	Φ_f	ns	10^8 s^{-1}	10^6 s^{-1}	cm^{-1}	cm^{-1}
298	0.001			56900[a]	15970	3163
273	0.002			28400[a]	16020	2959
243	0.003			18900[a]	16070	2806
228	0.005			11300[a]	16070	2653
213	0.009	0.16	0.563	6130	16070	2602
203	0.014	0.24	0.583	4040	16070	2500
193	0.017	0.42	0.404	2290	16120	2502
178	0.039	0.88	0.442	1040	16130	2503
163	0.075	1.85	0.405	450	16160	2503
143	0.200				16650	2449
123	0.300				17520	2449
108	0.350					

[a] Values calculated according to Eq. (7) and $k_f = 5.7 \cdot 10^8$ s^{-1}.

Table 5 Photophysical and spectroscopic data for *p*-DASPMI in ethanol at different temperatures.

T		τ_f	k_f	k_{nr}	ν_{max}^{flu}	$\nu_{1/2}^{flu}$
K	Φ_f	ns	10^8 s^{-1}	10^6 s^{-1}	cm^{-1}	cm^{-1}
298	0.008	0.051	1.51	19300	16270	2242
273	0.016	0.045	3.56	21500	16270	2185
243	0.036	0.14	2.57	6680	16330	2012
228	0.059	0.33	1.76	2660	16330	1925
213	0.097	0.62	1.56	1300	16380	1840
203	0.130	0.74	1.74	1030	16380	1725
193	0.190	1.21	1.57	541	16380	1725
178	0.300	2.1	1.43	216	16380	1725
163	0.400	2.57	1.56	106	16560	1725
143	0.450	2.87	1.57	63	17020	1897
123	0.480	2.85	1.68	45	17840	1878
108	0.500	2.45	2.04	37	17850	1676

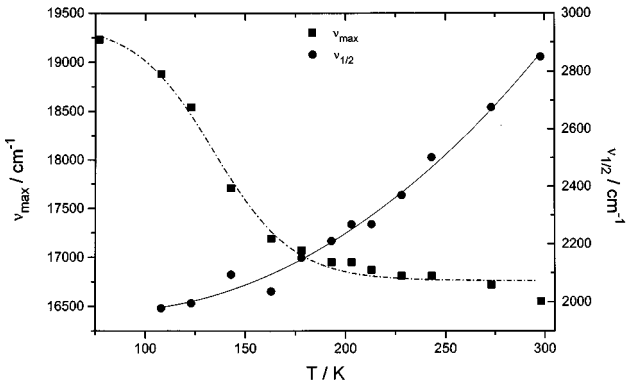

Fig. 8 Dependence of the fluorescence maximum ν_{max} and halfwidth of the spectra $\Delta\nu_{1/2}$ for *o*-DASPMI in ethanol at different temperatures.

involving solute relaxation.[46] Further analysis of this phenomenon can be gained by globally analyzing the fluorescence decay curves observed at different wavelengths. This can lead to the resolution of the spectra of individual species buried within the apparently single fluorescence band and will be shown in a subsequent paper.[23]

3. The anomaly of the fluorescence lifetime exhibiting a maximum at around 150 K (see Fig. 6) is not inherent in the solvent relaxation model. However, it can be understood by assuming that adiabatic photoreactions occur in the excited state, leading to several emissive species.[22] Former investigations of donor-acceptor stilbenes (4-dimethylamino-4′-cyano-stilbene, DCS) and other ring-bridged model compounds[19,20] indicate the validity of this assumption.
4. The wavelength and lifetime effects observed occur mainly in the high viscosity region and in the glassy state where the classical relaxation of solvent dipoles is nearly frozen and mainly the β-relaxation (relaxation of some molecular groups) of the matrix dominates.

In general, both theories—the relaxation of solvent dipoles[6,42,43] and the idea of several emitting states as discussed in this work—have to be taken into account to describe the fluorescence behavior of stilbenoid dyes. In the case of the DASPMI isomers, we believe that "multidimensional" photochemistry with several emitting states seems to dominate fluorescence behavior. On the other hand, the solvent relaxation model seems to gain more importance in nonionic donor-acceptor-substituted molecules. This different behavior can be viewed in relation to the fact that neutral molecules with large dipole moments in the excited state respond more strongly to changes of the dipolar properties of the solvent, whereas for charged molecules like the DASPMI compounds, the dipolar–solvent interaction is in part overwritten and masked by the strong monopolar contribution, which does not change upon excitation. Hence, the observed solvatochromic red shifts are only moderate.

3.3 DISCUSSION OF FREE VOLUME EFFECTS

The results discussed above show that the DASPMI compounds investigated in this work owe their medium sensitivity of the fluorescence to a complicated excited-state photochemistry. These compounds have received increased interest as fluorescence probes to describe changes in microviscosity and mobility. They possess the advantage of chemical inertness against nucleophiles[3] and of a satisfactory long-term photostability.[5] The most sensitive parameter is the temperature-dependent part of the nonradiative rate constant, k_{rot}, which is mainly influenced by the surrounding. In view of the anomalous fluorescence behavior of DASPMI, e.g. temperature-dependent k_f values, we chose to calculate k_{rot} using the following expression,

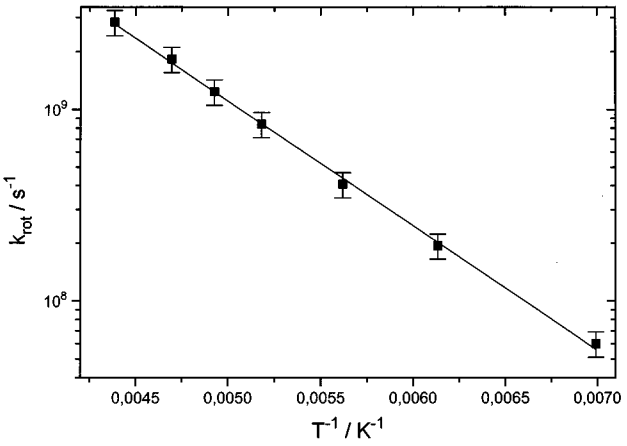

Fig. 9 Arrhenius plot for the nonradiative rate constant (k_{rot}) for *o*-DASPMI in the temperature region between 228 and 143 K (high viscosity region).

$$k_{rot} = k_f\left(\frac{1}{\Phi_f} - \frac{1}{\Phi_f(77\ K)}\right), \qquad (7)$$

which allows us to include explicitly the temperature dependence of k_f. The k_{rot} values calculated according to Eq. (7) are plotted logarithmically against the inverse temperature in Fig. 9 to determine the activation energy.

As can be seen from this plot, a good Arrhenius line is obtained in the temperature range between 143 and 228 K. The activation energy determined (12 kJ/mol) is smaller than the activation energy for viscous flow E_η for ethanol (15 KJ/mol[47]) in the temperature region investigated. Sometimes the movement into a "hole" of the relaxing free volume was discussed to explain such probe behavior in high viscous matrices.[7,27] Similar ideas were considered for the behavior of DASPMI in other matrices[3] and in the case of triphenylmethane dyes in glycerol[7] or aprotic oligomer systems.[27]

Moreover, the k_{rot} kinetics occurs on a nanosecond time scale (compare the data in Table 3 and Fig. 9). In terms of relaxation, they are situated in the so-called high-frequency domain (>1 MHz).[48] In this region, mainly the β-relaxation process of the solvent is monitored by the probe molecule. The β-relaxation corresponds to a relaxation of chain segments or clusters within a solvent or polymer,[49] and it shows usually a linear Arrhenius behavior. Typical rate constants for the β-relaxation are larger than 10^6 s^{-1}.[48,49] Similar linear dependencies have also been found for triphenylmethane dyes,[7,27] which are also present in the class of TICT molecules.[15,16] In all these cases, the rate constants for the formation of the photochemical product

states are all situated on a nanosecond time scale, and a linear Arrhenius behavior was found for these compounds. Furthermore, significant variations of the constant k_{rot} were also found in other polymer matrices,[3,27] that do not possess such strong hydrogen bonding interactions as the solvent ethanol.

In general, the results described offer many fields for applications of DASPMI as fluorescence sensors, although the sensitivity of k_{rot} is linked to a complicated adiabatic photochemical process that necessitates a mechanistic interpretation.

4 CONCLUSIONS

All the photophysical investigations in this work show that the DASPMI isomers possess interesting photophysical properties, which are a good basis for using these compounds as fluorescence probes for several applications, e.g., in polymer science[3] and medicine.[9–11]

First, *o*-DASPMI possesses a high photostability. This property is caused by the low trans→cis isomerization quantum yield ($<10^{-3}$ in ethanol at room temperature[5]) in contrast to substituted stilbenes with efficient trans→cis isomerization.[50] On the other hand, an efficient temperature-dependent nonradiative deactivation was observed and assigned to the population of single-bond twisted species in the excited state, which do not lead to permanent photoproducts after deactivation to the ground state. The molecular orbital structure of these dyes is related to that of unsymmetric cyanines.[51]

Second, the rate constants for nonradiative deactivation at viscosities ≤10 cP are comparable to solvent relaxation rate constants. In addition, a linear correlation was found for these rate constants on the solvent viscosity η. This means that all macroscopic changes of the surrounding are globally reflected in the changes of k_{nr}.

Third, the presence of several emitting species was demonstrated and can be correlated with the possible formation of single-bond twisted TICT excited states. They possess red-shifted spectra and a lower intrinsic k_f value than the near-planar species, which can be observed at 77 K. For application of the DASPMI isomers as fluorescence probes, however, it is helpful to consider the following aspects. Rotation around a double or a single bond requires a different free volume of the matrix, and the corresponding rate constants and temperature dependencies can be different, too. Scheme 2 illustrates the two different kinds of possible intramolecular rotational diffusion movements. The cylindrical movement of the phenyl group requires a smaller rotational volume than the conical rotation around the double bond. As a result, different rate constants for both processes will result, and are supposed to correlate with the microscopic mobility of this molecular moiety.

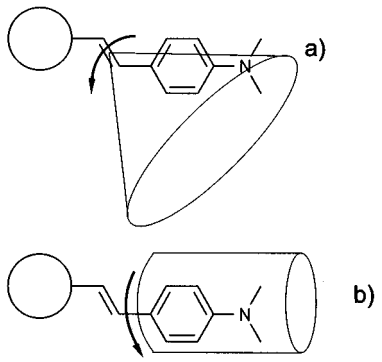

Scheme 2 The structure of the stilbazolium dyes investigated in this work and of stilbenoid dyes in general offers even more possibilities for adiabatic photoreactions. Rotation of both double and single bonds is possible. As can be seen from Scheme 2, rotation of the double bond (a) (conical movement) requires a larger volume in comparison to the rotation of a single bond (b) (cylindrical movement). The circle in this picture represents the acceptor part of the stilbenoid compound.

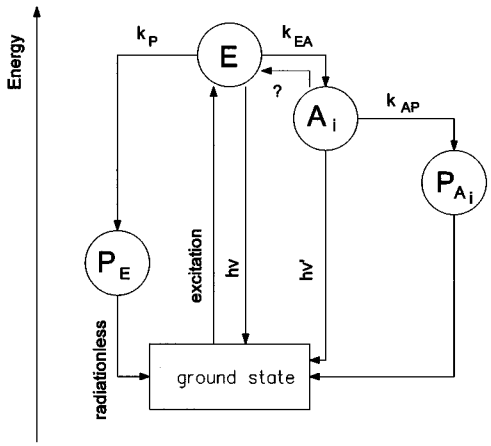

Scheme 3 Possible reaction scheme of DASPMI isomers based on a model for multiple fluorescence. After excitation, the state E* with planar geometry is formed. Two general kinds for an adiabatic photoreaction are possible: (1) A pure double-bond twist happens and the double-bond twisted state P_{E*} formed deactivates radiationless because of the very low energy gap between the ground and excited state; this route normally leads to trans-isomerization products, (2) A twist around one of the two single bonds i occurs. It is also possible that deactivation occurs before the perpendicular geometry is reached (especially in the case of P* conformers). The state A_i* formed has a sizeable energy gap to the ground state and can therefore also deactivate by fluorescence in the visible region, or it can be envisaged that a further state is reached photochemically by (partial) twisting around the double bond. This state, P_{Ai}*, may have a mainly nonradiative character. Upon arrival in the ground state, the partially twisted double bond may relax to the original planarity so that overall photochemical changes are not observed. This scheme predicts at least three emissive species: fluorescence from E*, two possible A_i* states, and, as an additional but faint possibility, from P_{Ai}*. In the simplest interpretation the experimental data are compatible with two emissive states.

Finally, an adiabatic photoreaction scheme is discussed on the basis of a model of multiple excited states (Scheme 3). This model is drawn from the known photochemical properties of stilbene and stilbenoid dye systems where the nonradiative channel is connected with the twisting process of the double bond. This property leads to a so-called "phantom-singlet" state P* with twisted double bond conformation. Since the formation process of P* involves a large amplitude twisting motion that displaces a large volume of solvent (movement a in Scheme 2), it is highly viscosity dependent, and consequently, the nonradiative decay rate, the fluorescence lifetime, and the quantum yields exhibit a strong viscosity dependence. On the other hand, the primarily excited E* state with planar geometry can also react by twisting around single bonds. By this coordinate, low-lying charge transfer states (A_i^*) can be formed where the positive charge of the cation is localized on the donor group, resulting in charge translocation or charge shift.[10] These states can be described within the TICT model.[14–16] Usually they possess more forbidden emissive character than E*. A CT state A_i* can deactivate by emission or it can be the intermediate step toward a further distortion of the molecule, e.g. involving double-bond twisting and leading to the conformation P_{Ai} (simultaneously twisted double and single bond). This species may be emissive, too. For molecules with such a rich possibility of photochemical pathways, a very powerful experimental tool is necessary, e.g. the technique of global analysis of fluorescence decay curves. This experimental method opens new ways for a better understanding of such compounds. More details about DASPMI and a global analysis of these results, together with quantum chemical calculations, will be presented in a subsequent paper.[23]

Acknowledgment

This work was supported by a Humboldt Fellowship to BS, and has been partially financed by the Bundesministerium für Forschung und Technologie (project 05 314 FAI5 and 05 5KT FAB9).

REFERENCES

1. S. P. Spooner and D. G. Whitten, "Photoreactions in monolayer films and Langmuir–Blodgett assemblies," in *Photochemistry in Organized and Constrained Media*, V. Ramamurthy, Ed., Chapter 15, pp. 691–739, VCH Publishers, Weinheim (1991).
2. A. Ulmann, *An Introduction to Ultrathin Organic Films - From Langmuir–Blodgett to Self-Assembly*, Chapters 3 and 5, Academic Press, San Diego (1991).
3. B. Strehmel, V. Strehmel, M. Younes, and S. Wartewig, "Time resolved fluorescence measurements during the curing of epoxy resins," *Prog. Coll. Polymer Sci.* **90**, 83–87 (1992).
4. H. Ephardt and P. Fromherz, "Fluorescence and photoisomerization of an amphiphilic aminostilbazolium dye as controlled by the sensitivity of radiationless deactivation to polarity and viscosity," *J. Phys. Chem.* **93**(22), 7717–7725 (1989).
5. H. Görner and H. Gruen, "Photophysical properties of quaternary salts of 4-dimethylamino-4'-azastilbenes and their quinolinium analogues in solution: IX," *J. Photochem.* **28**(3), 329–350 (1985).
6. D. Bringmann and N. P. Ernsting, "Femtosecond solvation dynamics determining the band shape of stimulated emission from a polar styryl dye," *J. Chem. Phys.* **102**(7), 2691–2700 (1995).
7. M. Vogel and W. Rettig, "Excited state dynamics of triphenyl-methane dyes for investigation of microviscosity effects," *Ber. Bunsenges. Phys. Chem.* **91**(11), 1241–1287 (1987).
8. D. Anwand, F.-W. Müller, B. Strehmel, and K. Schiller, "Determination of the molecular mobility and the free volume of thin polymeric films with fluorescence probes," *Makromol. Chem.* **192**(9), 1981–1991 (1991).
9. P. Fromherz, K. H. Dambacher, H. Ephardt, A. Lambacher, C. O. Müller, R. Neigl, H. Schaden, O. Schenk, and T. Vetter, "Fluorescent probes of voltage transients in neuron membranes," *Ber. Bunsenges. Phys. Chem.* **95**(11), 1333–1344 (1991).
10. L. M. Loew, S. Scully, L. Simpson, and A. S. Waggoner,"Evidence for a charge-shift electrochromic mechanism in probes of membrane potential," *Nature* **281**(5731), 497–499 (1979).
11. P. Fromherz and O. Schenk, "Voltage-sensitive fluorescence of amphiphilic hemicyanine dyes in a black lipide membrane of glycerol monooleate," *Biochim. Biophys. Acta* **1191**, 299–308 (1994).
12. H. Ephardt and P. Fromherz, "Anilinopyridinium: solvent-dependent fluorescence by intramolecular charge transfer," *J. Phys. Chem.* **95**(18), 6792-6797 (1991).
13. P. Fromherz and A. Heilemann, "Twisted internal charge transfer in (aminophenyl)pyridinium," *J. Phys. Chem.* **96**(17), 6964–6966 (1992).
14. Z. R. Grabowski, K. Rotkiewicz, A. Siemiarczuk, D. J. Cowley, and W. Baumann, "Twisted intramolecular charge transfer states (TICT). A new class of excited states with a full charge separation," *Nouv. J. Chim.* **3**(7), 443–454 (1979).
15. W. Rettig, "Charge separation in excited states of decoupled systems-TICT compounds and implications regarding the development of new laser dyes and the primary process of vision and photosynthesis," *Angew. Chem. Int. Ed. Engl.* **25**(11), 971–988 (1986).
16. W. Rettig, "Charge transfer in self-decoupling π-systems," in *Modern Models of Bonding and Delocalization: Molecular Structure and Energetics*, Vol. 6, J. Liebman and A. Greenberg, Eds., pp. 229–282, VCH Publishers, New York (1988).
17. U. Brackmann, *Lamdachrome Laser Dyes*, pp. 97, 252, Lamda Physik GmbH, Göttingen (1994).
18. R. Lapouyade, C. Czeschka, W. Majenz, W. Rettig, E. Gilalbert, and C. Rulliere, "Photophysics of donor-acceptor substituted stilbenes. A time resolved fluorescence study using selectively bridged dimethylamino model compounds," *J. Phys. Chem.* **96**(24), 9643–9650 (1992).
19. J.F. Létard, R. Lapouyade, and W. Rettig, "Structure property correlations in a series of 4-(dialkylamino)stilbenes: intramolecular charge transfer in the excited state as related to the twist around the single bonds," *J. Am. Chem. Soc.* **115**(6), 2441–2447 (1993).
20. W. Rettig, W. Majenz, R. Herter, J.F. Létard, and R. Lapouyade, "Photophysics of stilbenoid dye systems: a comparison of experiment and theory," *Pure Appl. Chem.* **65**(8), 1699–1704 (1993).
21. R. Lapouyade, A. Kuhn, J.F. Létard, and W. Rettig, "Multiple relaxation pathways in photoexcited dimethylaminonitro and dimethylaminocyanostilbenes," *Chem. Phys. Lett.* **208**(1–2), 48–58 (1993).
22. W. Rettig, W. Majenz, R. Lapouyade, and M. Vogel, "Adiabatic photochemistry with luminiscent products," *J. Photochem. Photobiol. A: Chem.* **65**(1–2), 95–110 (1992).
23. B. Strehmel and W. Rettig, to appear in *J. Phys. Chem.*
24. W. Rettig, M. Vogel, and A. Klock, "The time structure of synchrotron radiation as an experimental tool for versatile time-resolved measurements," *EPA Newsletters* **27**, 41–46 (1986).
25. T. Karstens and K. Kobs, "Rhodamine B and rhodamine 101 as reference substances for fluorescence quantum yield measurements," *J. Phys. Chem.* **84**(14), 1871–1872 (1980).
26. J. Heinze and U. Kopf, "2,7-bis(diethylamino)phena-

oxonium chloride as a quantum counter for emission measurements between 240–700 nm," *Anal. Chem.* **56**(11), 1931–1935 (1984).
27. B. Strehmel, V. Strehmel, H.-J. Timpe, and K. Urban, "Time resolved fluorescence measurements for the characterization of epoxy systems," *Eur. Polym. J.* **28**(5), 525–533 (1992).
28. D. V. O'Connor and D. Phillips, *Time-correlated Single Photon Counting*, Academic Press, London (1984).
29. K. Urban, "Aufbau, Funktionsweise und Testung einer zeitkorrellierten Einzelphotonenzählung," PhD thesis, Merseburg (1992).
30. W. Rettig, H. Wiggenhauser, T. Herbert, and A. Ding, *Nuclear Instr. Meth. Phys. Res.* **A277**, 677 (1989).
31. J. Del Bene and H.H. Jaffé, "Use of the complete neglet of differential overlap (C.N.D.O.) method in spectroscopy I." *J. Chem. Phys.* **48**(4), 1807–1813 (1968).
32. J. Del Bene and H.H. Jaffé, "Use of CNDO (complete neglect of differential overlap) method in spectroscopy II." *J. Chem. Phys.* **48**(9), 4050–4055 (1968).
33. L. E. Sutton, *Tables and Interatomic Distances and Configurations in Molecules*, The Chemical Society, London (1965).
34. W. Majenz, "Untersuchungen an Donor-Akzeptorsubstituierten Stilbenen und deren Derivaten," Ph.D. thesis, Technical University of Berlin (1991).
35. I. B. Berlmann, *Handbook of Fluorescence Spectra of Aromatic Molecules*, Academic Press, New York (1971).
36. N. J. Turro, *Modern Molecular Photochemistry*, Chapter 5, p. 87, Benjamin/Cummings, Menlo Park , CA (1978).
37. H. Hirata and N. Mataga, "Picosecond solvation dynamics of electrons in several alcohols," in *Dynamics and Mechanisms of Photoinduced Electron Transfer and Related Phenomena*, N. Mataga, T. Okada, and H. Masuhara, Eds., pp. 123–130, Elsevier, New York (1992).
38. M. L. Loew and L. L. Simpson, "Charge-shift probes of membrane potential. A probable electrochromic mechanism to p-aminostyrylpyridinium probes on a hemispherical lipid bilayer," *Biophys. J.* **34**(3), 353–365 (1981).
39. B. L. Anderson, J. M. Hoover, G. A. Lindsag, P. Stroeve, and S. T. Korvel, "Second harmonic generation in Langmuir-Blodgett multilayers of stilbazolium chloride polyethers," *Thin Solid Films* **179**, 413–421 (1989).
40. V. Strehmel and C.-W. Frank, "Synthesis and characterization of soluble oligoimides," *Polymer Preprints* **36**(1), 477–478 (1995).
41. M. Younes, S. Wartewig, D. Lellinger, B. Strehmel, and V. Strehmel, "The curing of epoxy resins as studied by various methods," *Polymer* **35**(24), 5269–5278.
42. J. P. Simon and S.-G. Su, "Solvation dynamics and the time dependent Stokes shift," *Proc. SPIE* **742**, 96–101 (1987).
43. S. Kinoshita, N. Nishi, and T. Kushida, "Dynamic Stokes shift in rhodamine 6G-ethanol solution," *J. Lumin.* **40–41**, 561–562 (1988).
44. W. Rettig, G. Wermuth, and E. Lippert, "Photophysical primary processes in solution of p-substituted dialkylanilines," *Ber. Bunsenges. Physik. Chemie* **83**(7), 692–697 (1979).
45. W. Rettig, "Intramolecular rotational relaxation of components which form intramolecular charge transfer (TICT) states," *J. Phys. Chem.* **86**(11), 1970–1976 (1982).
46. M. Van Damme, J. Hofkens, F.C. DeSchryver, T.G. Ryan, W. Rettig, and A. Klock, "Solvent dynamics and intramolecular charge transfer in 4-cyano-4'-butoxybiphenyl (4COB)," *Tetrahedron* **45**(15), 4693–4706 (1989).
47. P. S. Visvanath and G. Natarajan, *Databook on the Viscosity of Liquids*, Hemisphere, Washington (1989).
48. S. Matsuoka, *Relaxation Phenomena in Polymers*, Oxford Univ. Press, New York (1992).
49. G. A. Noyel, L. J. Jorat, O. Derriche, and J. R. Huck, "Dielectric properties of normal supercooled water in alcohol/water mixtures," *IEEE Trans. Elec. Insul.* **27**(6), 1136–1143 (1992).
50. D. H. Waldeck, "Photoisomerization dynamics of stilbenes," *Chem. Rev.* **91**(3), 415–436 (1991).
51. W. Rettig, B. Strehmel, and W. Majenz, "The excited states of stilbene and stilbenoid donor-acceptor dye systems," *Chem. Phys.* **173**(3), 525–537 (1993).